

COMBINED WAVE-CURRENT FORCES ON HORIZONTAL CYLINDERS

by

B.D. Chandler¹ and J.B. Hinwood²

ABSTRACT

Some early results are reported from an investigation of the forces exerted on horizontal cylinders by waves and currents. It appears that the values of the inertia coefficients decrease as U/u_0 increases, and the drag coefficients decrease also, for values of U/u_0 up to 0.7. Comparisons with measured data show that linear theory and the stream function theory satisfactorily describe the wave motion for the conditions investigated, and that velocity superposition can be used with either of these theories to describe conditions involving waves plus currents, with reasonable accuracy.

1. INTRODUCTION

There have been many theoretical and experimental investigations of the hydrodynamic forces that are exerted on submerged cylinders by wave action. Most have been aimed at deriving accurate values for the drag and inertia coefficients for use in the Morison force equation. The forces acting on a cylinder in a steady flow situation have also been investigated extensively, much of this work having been undertaken in wind tunnels. There has, however, been very little investigation of the forces that are exerted when there is a current present in addition to the waves.

Tung and Huang (1973) studied the importance of the presence of the current and the effects of wave-current interactions on the probability function, spectrum and peak distribution of the fluid loading on a cylinder. Since they were interested primarily in the effects of the current upon these statistical properties of the fluid

¹ Post Graduate Student, Department of Mechanical Engineering, Monash University, Clayton, Victoria, Australia.

² Associate Professor, Department of Mechanical Engineering, Monash University, Clayton, Victoria, Australia.

force, rather than in predicting actual force values for given situations, they assumed values for the Morison force coefficients. Dalrymple (1975) investigated the effects of combined waves and currents using field data obtained in the "Wave Project II" exercise. He concluded that the presence of a current must be taken into account in order to obtain accurate drag force coefficients. Knoll and Herlich (1980) conducted an experimental investigation of the simultaneous wave and current forces acting on a submerged pipeline. They found that the drag coefficients obtained from simultaneous measurement of the force and the velocity were less than those obtained when the velocity was computed by adding the wave velocity from Airy and Stokes third order wave theories to the current velocity. Recently, Kemp and Simons (1982) have undertaken an extensive experimental investigation of the wave/current kinematics. They found that the thickness of the steady flow boundary layer was reduced by the superposition of waves propagating with the current.

The purpose of the present study is to investigate the interaction that occurs between a known wave pattern and a known current; to determine the effects that this interaction has upon the hydrodynamic loading on a submerged, horizontal circular cylinder; and to relate the changes in loading to the detected flow pattern around the cylinder. Measurements were made of the water particle velocities in a combined wave-current flow condition. The wave-current interaction was investigated by comparing these measured values with the velocities obtained by vector addition of the individual wave and current components. One could thereby determine the accuracy achieved by representing the overall velocity field as the sum of the individual components. Measurements were also made of the forces acting on the cylinder; and these, together with the simultaneous velocity measurements, were used to calculate the force coefficients.

2. THEORY

2.1 Wave Theory

In this report, the principle of superposition is used for the theoretical prediction of fluid motion for conditions involving waves plus currents. The horizontal orbital velocities are therefore expressed as the sum of the current velocity and the orbital velocity predicted by the particular wave theory. For these calculations, the wave period used is the one measured in a frame of reference moving with the current. This period, denoted by T' , is defined as:

$$T' = T \left(\frac{V}{V - U} \right), \quad (1)$$

where T = wave period in stationary frame
 V = speed of propagation of wave crest in the flowing water
 U = current velocity (the average value over the cross-section of the channel).

The measurements will be compared with the predicted results of two wave theories: the Airy linear theory, and the stream function

theory. The stream function results are obtained from the tables prepared by Dean (1974). Linear interpolation is used to correct for the small departure of the wave parameters from the tabulated results.

2.2 Force Equation

The Morison (1950) equation is normally used for determining the hydrodynamic forces acting on a submerged cylinder due to wave action. In this equation, the force is expressed as the sum of a velocity-dependent drag force and an acceleration-dependent inertia force, as follows:

$$F = C_d \frac{1}{2} \rho D u \left| (u^2 + v^2)^{1/2} \right| + C_m \rho \frac{\pi D^2}{4} \dot{u} \quad (2)$$

where F = horizontal force per unit length
 ρ = density of fluid
 D = diameter of cylinder
 u = horizontal wave-induced water particle velocity
 v = vertical wave-induced water particle velocity
 \dot{u} = horizontal wave-induced water particle acceleration
 C_d = drag coefficient
 C_m = inertia coefficient.

The drag force term is commonly expressed as being proportional to $u|u|$; that is, independent of the vertical velocity. The definition given in eqn (2), however, more correctly describes the horizontal component of the total drag force acting on a horizontal cylinder.

Numerous investigations since 1950 have been aimed at determining the correct values to use for the drag and inertia coefficients. The results of these investigations show a considerable scatter in the derived values for the coefficients, and the coefficients have been shown to be dependent upon parameters such as the Reynolds number, the Keulegan-Carpenter period parameter, the surface roughness of the cylinder, and the vertical to horizontal velocity ratio, v/u .

The design codes (e.g. British Standards Institution (1978)) recommend that the velocities and accelerations be determined by using one of the commonly-used wave theories, such as the linear theory, the Stokes fifth order wave theory, or the stream function theory. The appropriate theory to use will depend upon the particular conditions at the site.

2.3 Force Equation for Simultaneous Waves Plus Current

For conditions involving waves as well as a current, the design codes recommend that the drag force term in the Morison equation be based upon the sum of the current velocity and the wave velocity which would be present in the absence of the current. For horizontal cylinders, the Morison equation should more accurately be written as follows:

$$F = C_d \frac{1}{2} \rho D(u + U) \left[((u + U)^2 + v^2)^{1/2} \right] + C_m \rho \frac{\pi D^2}{4} \dot{u} \quad (3)$$

where U = current velocity at the depth at which u and \dot{u} are being determined.

For the experimental analysis in this investigation, the term $(u + U)$ is replaced by the total, measured, horizontal velocity. Note that in eqn (3), F , u , v and \dot{u} are functions of time, varying over the wave period.

3. EXPERIMENTAL PROGRAMME

3.1 Equipment

The tests were conducted in a wave channel measuring 15 m in length, 0.60 m in width, and 0.30 m in depth. The waves were generated using a paddle driven by a variable speed electric motor. Openings in and under the paddle permitted the current to flow through it. A specially designed beach was used which satisfactorily dissipated the wave energy, while at the same time allowing water to flow through it. The beach face consisted of parallel wooden slats, with gaps between the slats equal to about 25% of the slat width. A layer of nylon filter material was placed over the upper surface of the slats. The slope of the beach was approximately 1 in 10.

The aluminium test cylinders were 400 mm long, with phosphor bronze end plates fitted to each end. Two different cylinders were used; one having a diameter of 12.7 mm, and the other having a diameter of 25.4 mm. The hydrodynamic forces acting on the cylinder were measured with load-cell devices attached to each end of the cylinder. The load-cells employed semiconductor strain gauges arranged in a Wheatstone Bridge configuration, which had the advantages of increasing the signal output as well as rendering the devices insensitive to small temperature fluctuations. The load cells were tested and found to have negligible drift over a typical recording period of a few hours. Both the vertical and the horizontal forces acting on the cylinder could be measured and recorded simultaneously. To avoid possible errors, no mechanical damping was incorporated into the load cells. They were therefore vulnerable to external mechanical vibrations. To overcome this problem, a very rigid support was constructed for the test assembly, and the support was isolated from the parts of the laboratory building which could transmit vibrations.

A 2 W Argon-Ion laser-Doppler velocimeter was used to measure the water particle velocities. This enabled the horizontal and vertical velocity components to be measured simultaneously, at a point at the same relative depth as the test cylinder.

Two capacitance-type wave gauges were used to measure the water surface elevation directly above the velocity measurement point and above the test cylinder.

The laboratory's constant head tank was used to supply the water for the experiments requiring a current. The head tank was connected, via a control valve, to a reservoir behind the paddle. After flowing through the paddle, along the channel and through the beach, the water passed over a control weir into a weighing tank. It then flowed into the laboratory's sump, from which it was pumped back up to the head tank. The weighing tank was used to obtain an accurate measure of the mass flow rate of the current, from which one could easily determine the current velocity, averaged over the cross-section of the channel.

3.2 Procedure

The still water depth for all tests was 220 mm. The horizontal test cylinders were positioned at three different levels, namely 60, 100 and 150 mm above the floor of the channel. The lowest level was therefore 2.4 cylinder diameters above the floor of the channel, whilst the upper level was nearly 3 diameters beneath the still water level. These levels were set to ensure that no interference effects would occur as a result of the proximity of these boundaries.

The experiments involved generating waves of the same height and period on four different current velocities, ranging from 0 to approximately 100 mm/s. The experiments were repeated for waves of different heights and periods. Four different periods were used, ranging from 0.72 to 1.25 s, with two different heights, ranging from 40 to 74 mm, for each period.

In each experiment, six channels of data were recorded simultaneously. These were the horizontal and vertical forces acting on the cylinder; the horizontal and vertical velocities being measured by the laser-Doppler; and the water levels directly above the cylinder and the velocity measurement point. The velocity measurement point was normally about 150 mm upstream from the cylinder.

A sampling rate of 1000 Hz was used to record the six channels of data, and so each variable was sampled at approximately 167 Hz. The minimum number of measurements for each wave cycle was therefore 120. Data were sampled for approximately 30 seconds, corresponding to 24 to 43 successive wave cycles per sample. All measurements were immediately digitised and stored on magnetic disc for subsequent analysis on an HP21MX computer. The resolution of the analog to digital converter was 5 mV, which was satisfactory in view of the fact that the signal inputs were all of the order of a few volts.

Measurements were made of the time taken for the waves to travel 7.8 m along the channel. From this, one could determine the wave celerity, the wavelength (from knowing the period), and also the phase shift between the locations of the velocity measurement point and the test cylinder.

The load cells were calibrated each day, with the cylinder set up in the configuration being used for that day's experiments. The

calibration of the laser-Doppler was checked on several occasions throughout the course of the experiments; and the wave gauges were calibrated several times at the end of the experiments. No significant changes in the calibration factors were observed for any of the instruments.

3.3 Range of Parameters

The ranges of wave heights and periods, and the current velocities, have already been given in Section 3.2. The still water depth and the steady flow depth was 220 mm for all experiments.

The experiments covered the following ranges of dimensionless parameters:

$$\frac{U}{u_o} : 0 \text{ to } 1.2$$

$$K : 2.1 \text{ to } 14.2$$

$$Re : 9 \times 10^2 \text{ to } 5 \times 10^3$$

$$\frac{v_o}{u_o} : 0.23 \text{ to } 0.86$$

$$\frac{H}{L_o} : 0.015 \text{ to } 0.069$$

$$\frac{h}{L_o} : 0.080 \text{ to } 0.272$$

$$\frac{H}{H_b} : 0.23 \text{ to } 0.43$$

where h = still water depth
 H = wave height
 H_b = breaker height = $0.78 h$
 u_o = horizontal velocity amplitude
 v_o = vertical velocity amplitude
 K = Keulegan-Carpenter number = $u_o T/D$
 L_o = deep water wavelength
 Re = Reynolds number (based on u_o).

3.4 Data Reduction

The drag and inertia coefficients, as defined in eqn (3), were determined by least squares curve-fitting over one whole wave cycle. The average values of the drag and inertia coefficients for each flow condition were obtained in two different ways. One method involved calculating the coefficients for each wave cycle sampled, and determining the average value of these 20 to 40 coefficients. The other method involved averaging the velocity, acceleration and force

data from the 20 to 40 wave cycles sampled, to obtain one representative cycle for each variable, for that particular flow condition. The drag and inertia coefficients were then determined from these averaged cycles of the velocity, acceleration and force. As would be expected, no significant differences were found between the values of the coefficients calculated by these two different methods. These averaged cycles of data were also used for all comparisons of profiles, velocities and accelerations with the wave theories.

4. RESULTS

4.1 Forces

One of the aims of this study is to investigate the effects that the introduction of a steady flow velocity component has upon the values of the drag and inertia coefficients. Figs. 1 and 2 show some of the results obtained by plotting the force coefficients against the current/wave velocity ratio U/u_0 . The points lying on each series of lines have approximately the same values of K and v_0/u_0 . The results shown are for the 25 mm diameter cylinder, for the levels 98 mm and 148 mm above the floor of the channel. The results for the 12.7 mm diameter cylinder showed similar trends to the larger cylinder, but there were unexpected inconsistencies between the three different levels. These experiments are presently being repeated, and so no results are yet available.

It can be seen in Fig. 1 that the values of C_m decrease steadily as U/u_0 increases, such that when $U/u_0 = 1.0$, the values of C_m are about 0.4 less than for $U/u_0 = 0$. The values of K range from 2.3 to 7.6, and v_0/u_0 ranges from 0.35 to 0.82. Both of these parameters appear to have had little influence on the value of C_m , over the ranges quoted.

In Fig. 2, the values of C_d decrease rapidly as U/u_0 increases from 0 to about 0.7. Then the values increase rapidly as U/u_0 increases from 0.7 to 1.1. The reasons for this dramatic change are not clear. It was observed, however, that, for conditions in which U/u_0 was approximately 1.0, the force records displayed a periodic behaviour whose period was twice that of the wave period. This may have been caused by a regular, asymmetric vortex shedding pattern, and it is proposed to investigate this further with the assistance of hydrogen bubble flow visualisation. If a vortex shedding pattern is causing the two-period variation in the force records as well as the change in the C_d values, then it is surprising that it appears to have had negligible effect upon the values of C_m .

The ranges of K and v_0/u_0 for the results shown in Fig. 2 are the same as those for Fig. 1, and once again these two parameters appear to have had little effect on the value of C_d .

The values obtained for both coefficients were compared with those reported by others for conditions involving waves alone. They

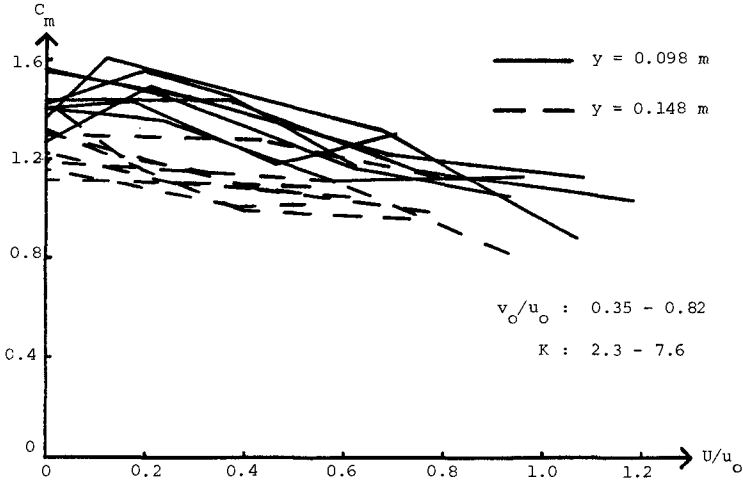


Fig. 1 C_m vs. U/u_o

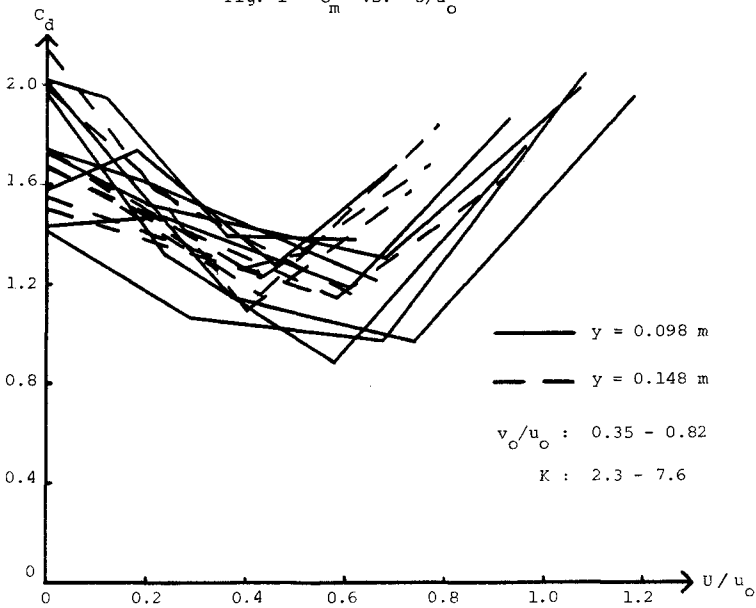


Fig. 2 C_d vs. U/u_o

were generally within the range bounded by the results obtained by Ramberg and Niedzwecki (1980), and the planar flow water tunnel results obtained by Sarpkaya, as reported by the previous authors. There was a slight tendency for the coefficients obtained for high values of U/u_0 to be closer to Sarpkaya's results.

The error analysis technique developed by Dean (1976), and modified by Chandler and Hinwood (1981) to apply to conditions involving waves plus a current, was used to determine the suitability of the experimental data for determining the drag and inertia coefficients. Generally, the experiments involving waves alone were better suited for determining the inertia coefficients. As the current velocity was increased, the drag force became more dominant until, for the maximum current speeds investigated, the data had become better conditioned for determining C_d than C_m .

4.2 Wave Motion

4.2.1 Description of Wave Data

All of the experimental results presented in this section are averaged results, obtained by averaging the data from at least ten successive wave cycles. For the comparisons of experimental results with theoretical results, the phase-matching of the different curves was done subjectively to achieve the best general fit over the whole cycle, rather than just matching the curves at, for instance, the crests.

The same basic wave pattern was used for all of the comparisons presented. The main features of this wave pattern are as follows: $H = 0.073$ m ; $h = 0.220$ m ; $T = 0.83$ s (measured in the stationary reference frame); $L = 0.968$ m ; $C = 1.166$ m/s ; $h/L_0 = 0.205$; $H/L_0 = 0.068$; $H/h_0 = 0.43$. For these conditions, Dean (1974) suggests that Stokes V would be the analytical theory providing the best fit to the dynamic free surface boundary condition, but that the stream function V theory would be the best theory overall. For the conditions involving waves plus current, the average current velocity across the channel was 101 mm/s for Figs. 3 and 4, and 61 mm/s for Figs. 5 to 8.

Similar comparisons have been done for a wave pattern with $H = 0.047$ m , $T = 1.03$ s and $L = 1.310$ m . The results are not shown in this report, but the observed trends and wave theory comparisons were found to be similar to those presented.

For the linear theory predictions for waves plus current, the calculations were based on the measured wave height, the measured wavelength, and the period measured in the frame of reference moving with the current, as described in eqn (1). The average current velocity (61 mm/s) was added to the calculated horizontal orbital velocity.

For the stream function predictions of waves plus current, the wave conditions were determined from the appropriate values of h/L_0

and H/L_0 , where L_0 was set equal to the speed of propagation of the wave in deep water multiplied by the period measured in the stationary reference frame. The speed of propagation was calculated as the sum of the deep water wave celerity for the wave period measured in the moving reference frame, and the average current velocity. Once again, the average current velocity (61 mm/s) was added to the calculated horizontal orbital velocity.

The measured velocities were all measured at a point 100 mm in from the side wall of the channel, and approximately 100 mm above the floor of the channel. The velocities were also measured 300 mm in from the wall, which is effectively in the middle of the channel, but these measurements were not used here since the laser-Doppler signals had higher noise levels than those obtained nearer the wall. Comparisons were made between data measured at these two locations, and it was found that there was no significant difference between them.

For the data presented in this report, the positive direction for the horizontal velocities is the direction of wave propagation. For the vertical velocities, positive is taken as being upwards. The surface elevations are also positive upwards.

4.2.2 Wave Profiles

Fig. 3 shows a comparison of the wave profiles for waves of identical height and period (measured in the stationary frame), one being for waves alone, and the other being for waves plus a current of 101 mm/s. The introduction of the current lowered the levels of both the trough and the crest by about 6% of the wave height, and the trough was not as flat and shallow as for the zero flow case. The current also made the leading face of the wave flatter, and the trailing face slightly steeper.

Figs. 5 and 6 show comparisons of the measured profiles with the linear theory and stream function theory profiles, for conditions involving waves alone and waves plus a current of 61 mm/s. For both flow conditions, the measured crests and troughs laid well above the linear theory predictions. For the zero flow case, the differences were about 8% of the wave height, while for waves plus current the differences were about 6%. The measured profiles had flatter troughs, and narrower, steeper crests than the sinusoidal profiles.

For waves alone, the stream function profile compared extremely well with the measured profile. The measured crest and trough were about 1% below the predicted levels, and the general shape of the wave was almost identical. For the wave plus current condition, the measured crest and trough were about 4% below the stream function levels, and there was still reasonably good agreement between the shapes of the two profiles.

The stream function profiles provided better predictions of the extreme water levels and water surface slopes than did the linear theory profiles, although the linear ones were still only about 8% to

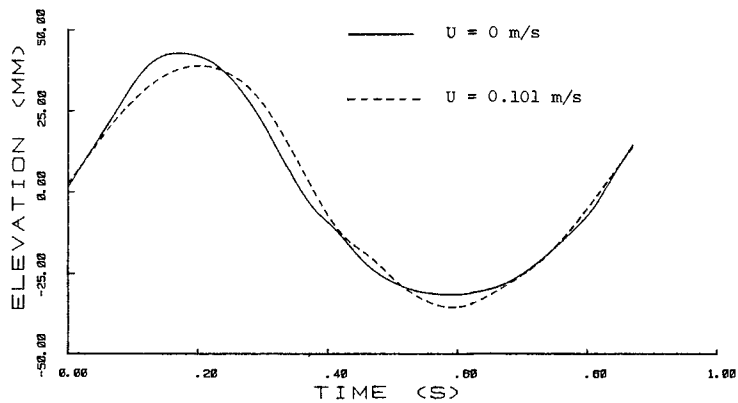


Fig. 3 Comparison of measured wave profiles
(H = 0.074 m, T = 0.83 s, y = 0.098 m)

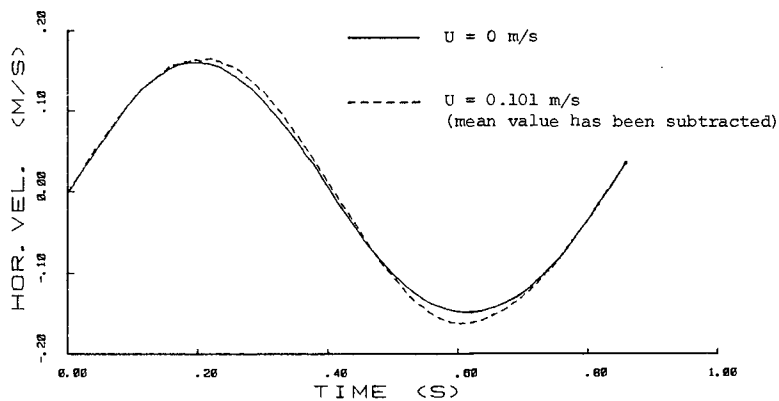


Fig. 4 Comparison of measured horizontal velocities
(H = 0.074 m, T = 0.83 s, y = 0.098 m)

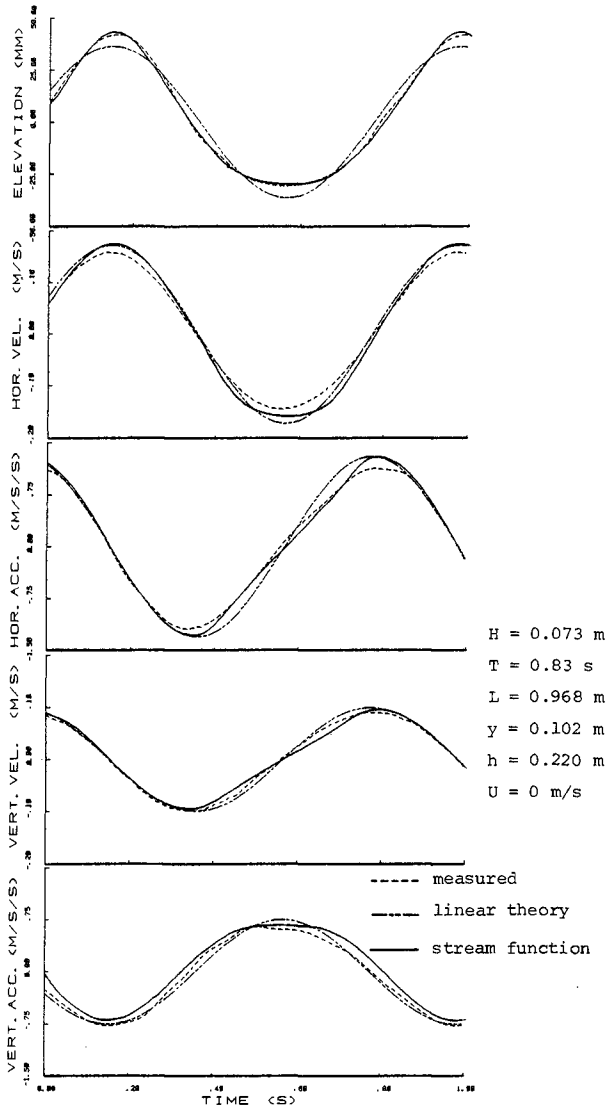


Fig. 5 Comparisons of measured and predicted values for waves alone

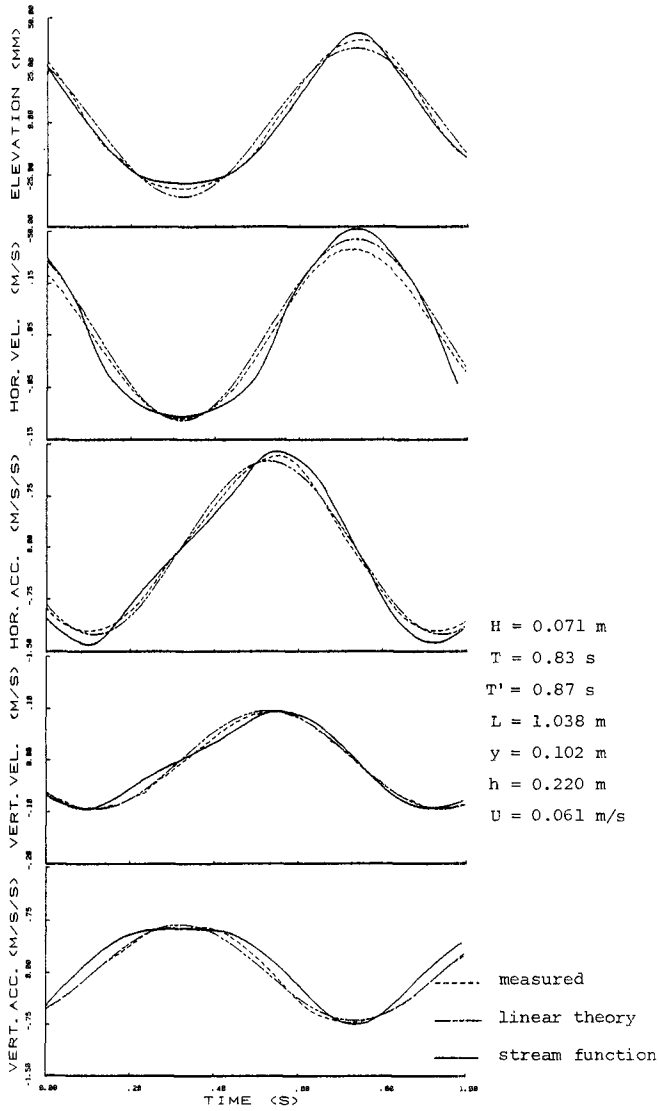


Fig. 6 Comparisons of measured and predicted values for waves plus current

10% of the wave height in error. The linear theory improved slightly for the waves plus current condition, whereas the stream function became slightly worse.

4.2.3 Velocities

Fig. 4 shows a comparison of the measured horizontal velocities for waves alone and for waves plus current. The average current over the cross-section of the channel was 101 mm/s, and the wave celerity for the zero flow condition was 1161 mm/s. The mean velocity over one cycle for the waves plus current condition at the point of measurement was 99 mm/s, and this has been subtracted from the velocities so that both curves have zero mean. The shapes of the two curves are very similar, but the waves plus current curve has a range about 6% greater than the waves only case. However, if linear theory corrections are applied to correct for the period measured in the moving reference frame and also the longer wavelengths of the waves on the current, then this reduces the waves plus current velocities by 6%, making the amplitudes of the two curves almost identical.

Figs. 5 and 6 show comparisons of the measured horizontal velocities with linear theory and stream function predictions. For waves alone, both theories gave similar velocity curves, and they both overestimated the peak velocities. The stream function theory overestimated the velocity range by about 10%, whilst the linear theory overestimated it by about 13%. For the waves plus current conditions, the stream function overestimated the range by about 10%, whereas the linear theory was only about 7% too great.

Figs. 7 and 8 show the variation with depth of the peak horizontal velocity, for y/h varying from 0 to 0.7, where y is the height above the floor of the channel. Due to limitations of the laser-Doppler traversing rig, velocity measurements could not conveniently be obtained at levels higher than $y/h = 0.7$. Fig. 7 indicates that for waves alone, both theories overestimated the velocity range, over most of the depth, by about 5% to 12%, with the stream function theory being generally slightly better. For the waves plus current conditions in Fig. 8, the mean values of the measured results became less than the average mean of 61 mm/s, as y/h increased. This suggests that there may have been a net circulation or drift set up in the channel, in addition to the steady flow. Looking at the velocity range, however, both theories once again overestimated the range by 5% to 15%. In this case the linear theory appears to have provided the better overall estimate.

Figs. 5 and 6 also show comparisons of measured vertical velocities with the theoretical estimates. Generally the agreement is very good. For waves alone, the peak downward velocities were predicted to within a few percent by both theories, and the peak upward velocities were overestimated by both theories, by up to about 5% for the linear theory. Overall, the stream function provided a better estimate. For waves plus current, the two predicted ranges were virtually the same as the measured range. The linear theory provided a slightly better fit at points between the peaks.

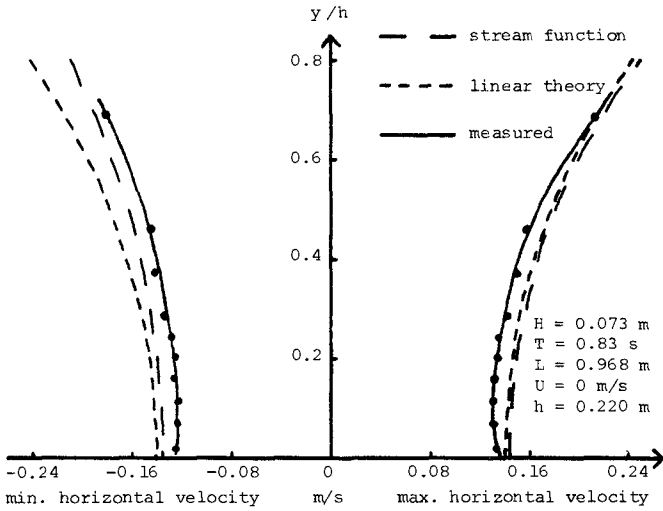


Fig. 7 Variation with Depth of Peak Horizontal Velocity - Waves Alone

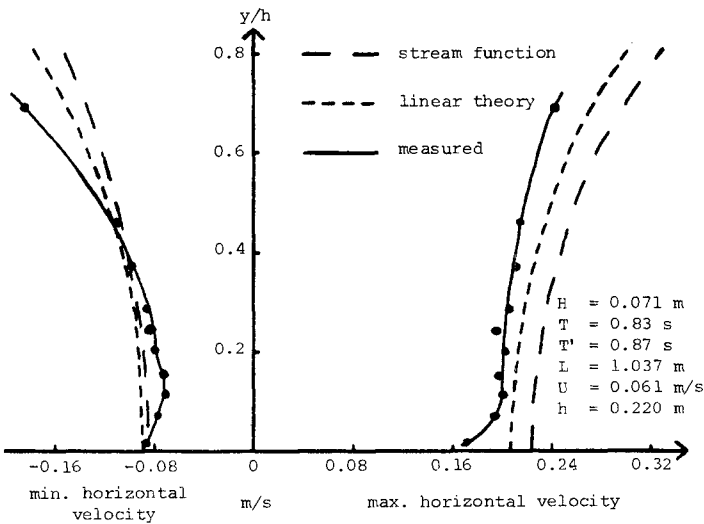


Fig. 8 Variation with Depth of Peak Horizontal Velocity - Waves Plus Current

4.2.4 Accelerations

Figs. 5 and 6 show comparisons of measured and predicted horizontal and vertical accelerations, for waves alone and waves plus current. In Fig. 5, for waves alone, both theories overestimated the peak horizontal accelerations. The linear theory overestimated the range by about 12%, and the stream function theory was about 10% too great. The stream function generally provided the better estimate.

For the case of waves plus current, (Fig. 6), the linear theory slightly overestimated the negative horizontal acceleration peak and underestimated the positive peak, so that its estimated range was only about 1% less than the measured range. The stream function theory overestimated the negative peak appreciably, and slightly overestimated the positive peak, so that its estimated range was about 9% greater than the measured range.

The linear theory's prediction of the vertical acceleration, for waves alone, slightly underestimated the downward accelerations at the wave crest, and overestimated the upward accelerations at the trough by about 7%. This is consistent with the fact that the measured wave profiles had wider, flatter troughs than the sinusoidal profile. The stream function slightly underestimated the crest accelerations, and overestimated the trough accelerations, such that its estimated range was approximately the same as the measured range.

For the vertical acceleration for waves plus current, both theories estimated the peaks and the range to within a few percent. The linear theory, however, provided the better estimate of the general shape of the acceleration curve.

5. CONCLUSION

This paper reports some of the early results obtained from a continuing investigation of the forces exerted on submerged horizontal cylinders by wave and current action. The range and conditions of the experiments were limited, with Keulegan-Carpenter numbers ranging from 2 to 14 and Reynolds numbers ranging from 900 to 5000, based on the orbital velocities. Due to the small scale of the experiments, it cannot be hoped to be able to use the experimental results to recommend coefficient values for prototype conditions. However, it is hoped to be able to provide a greater understanding of the forces exerted by interacting waves and currents, and in particular how these forces and the force coefficients compare with those for waves alone.

Early results from the force data analysis suggest that the values of the inertia coefficient decrease as the current velocity ratio U/u_0 increases. Typically, the coefficients decrease from a value of about 1.4, at $U/u_0 = 0$, to about 1.0 at $U/u_0 = 1.0$. The drag coefficients initially decrease as U/u_0 increases to about 0.7, and then they increase again, as U/u_0 goes from 0.7 to 1.1. As already discussed, this change in behaviour may be attributable to a dominant vortex shedding phenomenon.

The measured water surface elevations, water particle velocities and accelerations for conditions involving waves alone and also waves plus current have been compared with the results predicted by the Airy linear theory and the fifth order stream function theory. The wave conditions, which extend to $H/H_D = 0.43$, are such that the linear theory would not be expected to be very accurate. It is found that the stream function theory provides better estimates of the elevation, velocities and accelerations, for conditions involving waves alone. Often, it is only marginally better than the linear theory, and the maximum errors associated with the linear theory are only about 10%. For conditions involving waves plus current, the linear theory generally provides a better estimate of the velocities and accelerations than does the stream function. The maximum errors for either theory are still normally less than 10% of the measured value. Both theories can therefore be used with reasonable accuracy for the types of wave conditions investigated here. It would also appear that velocity superposition is valid for both theories, for describing wave plus current conditions.

6. REFERENCES

- BRITISH STANDARDS INSTITUTION (1978). Draft for development; fixed offshore structures.
- CHANDLER, B.D. and HINWOOD, J.B. (1981). The hydrodynamic forces on submerged horizontal cylinders due to simultaneous wave and current action. Proc. 5th Aust. Conf. on Coastal and Ocean Eng., pp 108-115.
- DALRYMPLE, R.A. (1975). Waves and wave forces in the presence of currents. Civil Engineering in the Oceans, Vol. 2, pp 999-1018.
- DEAN, R.G. (1974). Evaluation and development of water wave theories for engineering application, Vols. I and II. U.S. Army, Corps of Eng., C.E.R.C.
- DEAN, R.G. (1976). Methodology for evaluating suitability of wave and wave force data for determining drag and inertia coefficients. Proc. Behaviour of Offshore Structures, pp 40-64.
- KEMP, P.H. and SIMONS, R.R. (1982). Wave and current interaction in the near bed region. Abstracts, 18th Int. Conf. on Coastal Eng., Cape Town, pp 240-241.
- KNOLL, D.A. and HERBICH, J.B. (1980). Wave and current forces on a submerged offshore pipeline. 12th Offshore Technology Conference, 1980, Paper No. 3762.
- MORISON, J.R., O'BRIEN, M.P., JOHNSON, J.W. and SCHAAP, S.A. (1950). The force exerted by surface waves on piles. Petroleum Transactions, AIME, Vol. 189, pp 149-154.

RAMBERG, S.E. and NIEDZWECKI, J.M. (1980). The sensitivity of wave force computations to common errors, uncertainties, and hydrodynamic approximations. NRL Memorandum Report 4206.

TUNG, C.C. and HUANG, N.E. (1973). Combined effects of current and waves on fluid force. Ocean Engineering, Vol. 2, pp 183-193.